CHEMISTRY
A EUROPEAN JOURNAL

DOI: 10.1002/chem.201000522

Modular, Homochiral, Porous Coordination Polymers: Rational Design, Enantioselective Guest Exchange Sorption and Ab Initio Calculations of Host–Guest Interactions

Danil N. Dybtsev,[a, b] Maxim P. Yutkin,[a] Denis G. Samsonenko,[a] Vladimir P. Fedin,*[a] Alexey L. Nuzhdin,[c] Andrey A. Bezrukov,[c] Konstantin P. Bryliakov,[c] Evgeniy P. Talsi,[c] Rodion V. Belosludov,[d] Hiroshi Mizuseki,[d] Yoshiyuki Kawazoe,[d] Oleg S. Subbotin,[a] and Vladimir R. Belosludov[a]

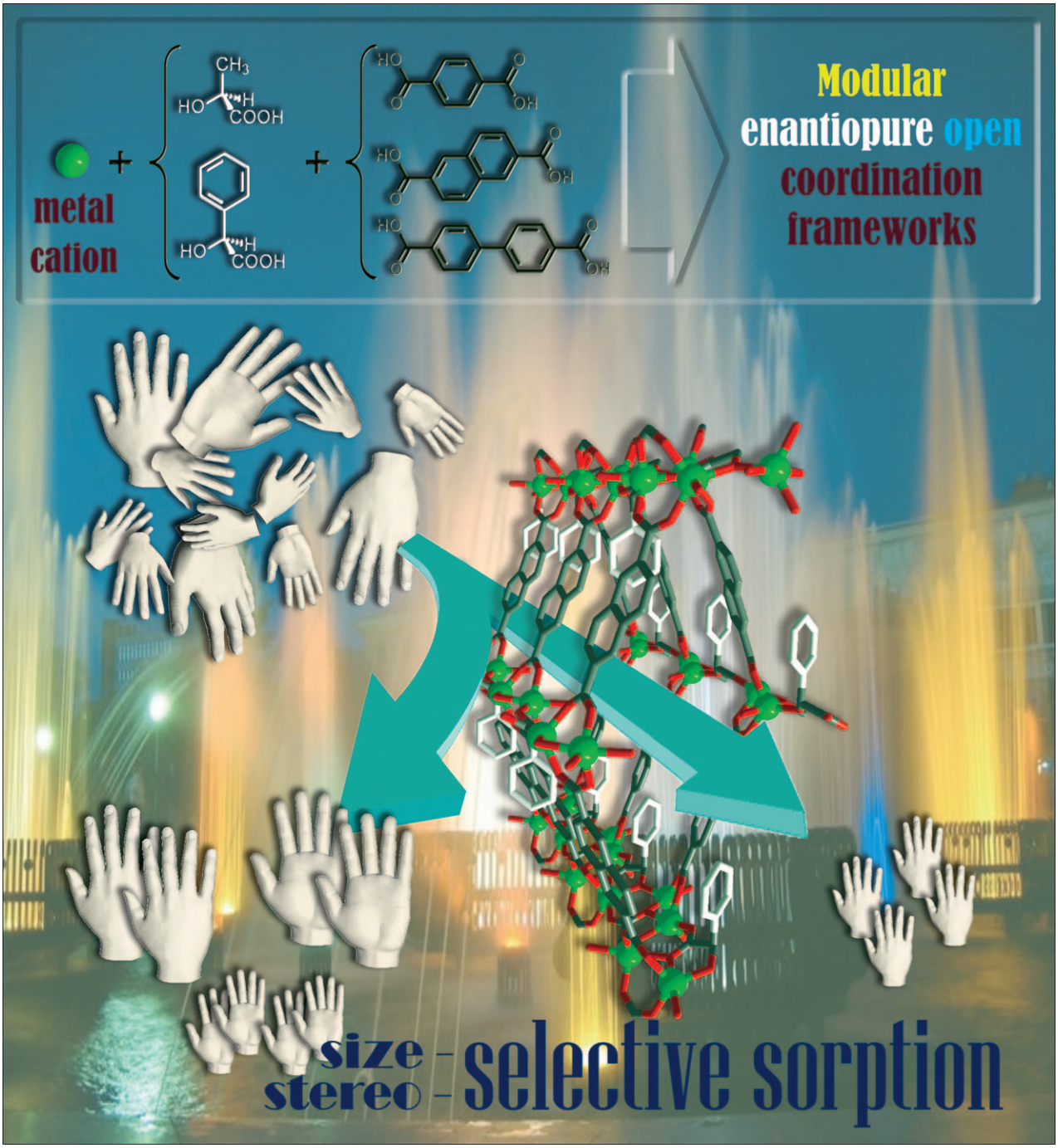

Abstract: Two new, homochiral, porous metal–organic coordination polymers $[Zn_2(ndc)\{(R)\text{-man}\}(dmf)]\cdot 3DMF$ and $[Zn_2(bpdc)\{(R)\text{-man}\}(dmf)]\cdot 2DMF$ (ndc = 2,6-naphthalenedicarboxylate; bpdc = 4,4′-biphenyldicarboxylate; man = mandelate; dmf = *N*,*N*′-dimethylformamide) have been synthesized by heating Zn^{II} nitrate, H_2ndc or H_2bpdc and chiral (*R*)-mandelic acid (H_2man) in DMF. The colorless crystals were obtained and their structures were established by single-crystal X-ray diffraction. These isoreticular structures share the same topological features as the previously reported zinc(II) terephthalate lactate $[Zn_2(bdc)\{(S)\text{-lac}\}(dmf)]\cdot DMF$ framework, but have larger pores and opposite absolute configuration of the chiral centers. The enhanced pores size results in differing stereoselective sorption properties: the new metal–organic frameworks effectively and stereoselectively (*ee* up to 62%) accommodate bulkier guest molecules (alkyl aryl sulfoxides) than the parent $[Zn_2(bdc)\{(S)\text{-lac}\}(dmf)]\cdot DMF$, while the latter demonstrates decent enantioselectivity toward precursor of chiral anticancer drug sulforaphane, $CH_3SO(CH_2)_4OH$. The new homochiral porous metal–organic coordination polymers are capable of catalyzing a highly selective oxidation of bulkier sulfides (2-NaphSMe ($2\text{-}C_{10}H_7SMe$) and $PhSCH_2Ph$) that could not be achieved by the smaller-pore $[Zn_2(bdc)\{(S)\text{-lac}\}(dmf)]\cdot DMF$. The sorption of different guest molecules (both *R* and *S* isomers) into the chiral pores of $[Zn_2(bdc)\{(S)\text{-lac}\}(dmf)]\cdot DMF$ was modeled by using ab initio calculations that provided a qualitative explanation for the observed sorption enantioselectivity. The high stereo-preference is accounted for by the presence of coordinated inner-pore DMF molecule that forms a weak C–H···O bond between the DMF methyl group and the (*S*)-$PhSOCH_3$ sulfinyl group.

Keywords: chirality · density functional calculations · metal–organic frameworks · porous materials

Introduction

Chirality is one of the major phenomena in nature, since most biological processes involve chiral reactants and catalysts, and hence biological evolution is entirely dependent on the occurrence of chiral recognition and catalysis. In the last decades, the chemistry of chiral compounds has expanded greatly, following the growing world's demand for optically pure compounds. Tremendous research efforts have been invested into the synthesis of artificial chiral polymers,[1] which has resulted in the emergence of a new class of compounds, homochiral porous metal–organic polymers,[2] which have the following attractive properties: versatile design opportunities as well as potential applications for stereoselective sorption and catalysis.[3,4]

The importance of such potential applications is clear, providing that the main consumers of synthetic chiral compounds (such as pharmaceutical, cosmetic, agrochemical industries etc.[5]) often require that such chemicals should be present as single stereoisomers.[6,7] This means that for chiral compounds obtained by various synthetic methods, subsequent purification is required to enrich them with the desired stereoisomer. Enantioselective sorption and chromatography are known, simple, and reliable methods for both stereoselective resolution and fine purification of optical isomers. To date, most chiral stationary phases are based on polysaccharide derivatives immobilized on silica gel. Recent work has demonstrated the high potential of enantiopure (homochiral) porous coordination polymers as a new class of chiral sorbents, capable of high stereoselectivity in catalysis,[8] sorption[3,4,9,10] and chromatographic separation[11] of racemic mixtures.

Versatility of design of metal–organic structures is another advantage of this class of compounds, allowing customization of the size and chirality of the pore structures for a particular chiral guest.[1] Despite these advantages, the availability of starting chiral materials and the synthesis of the porous structure remain challenging problems for homochiral coordination polymers. Fine-tuning of the pore size, shape, and other structural features in the chiral frameworks is an especially important task, which has been solved with limited success.[12–14]

Recently we have introduced a new approach for the synthesis of porous homochiral coordination polymers, which has resulted in a series of isoreticular zinc(II) camphorates of similar structures with chiral centers and tunable pore size.[13] In an earlier example, a simple one-pot reaction of

[a] Prof. Dr. D. N. Dybtsev, M. P. Yutkin, Dr. D. G. Samsonenko, Prof. Dr. V. P. Fedin, Dr. O. S. Subbotin, V. R. Belosludov
Nikolaev Institute of Inorganic Chemistry
Siberian Branch of the Russian Academy of Sciences
Pr. Lavrentieva 3, 630090 Novosibirsk (Russian Federation)
Fax: (+7) 383-3309489
E-mail: cluster@niic.nsc.ru

[b] Prof. Dr. D. N. Dybtsev
Division of the Advanced Materials Science, POSTECH
San 31, Hyojadong, 790-784 Pohang (Republic of Korea)

[c] Dr. A. L. Nuzhdin, A. A. Bezrukov, Prof. K. P. Bryliakov, Prof. E. P. Talsi
Boreskov Institute of Catalysis
Siberian Branch of the Russian Academy of Sciences
Pr. Lavrentieva 5, 630090 Novosibirsk, (Russian Federation)

[d] Prof. R. V. Belosludov, Prof. H. Mizuseki, Prof. Y. Kawazoe
Institute for Materials Research
Tohoku University
Katahira 2-1-1, 980-8577 Sendai (Japan)

Supporting information for this article is available on the WWW under http://dx.doi.org/10.1002/chem.201000522.

readily available chemicals produced the zinc(II) terephthalate lactate $[Zn_2(bdc)(lac)(dmf)]$ (bdc = terephthalate, lac = (*S*)-lactate dianion, dmf = *N*,*N*′-dimethylformamide)—a homochiral porous coordination polymer with a pore size of about 5 Å.[10] This structure exhibited acceptable catalytic activity and selectivity in sulfide oxidation to sulfoxides as well as remarkable size and enantioselective sorption properties toward chiral sulfoxides.[10] More importantly, porous zinc(II) terephthalate lactate was further utilized as a chiral stationary phase for the semipreparative, enantioselective chromatographic resolution of racemic sulfoxides.[11a] However, the relatively small pore size of the chiral polymer hampered the effective enantioseparation of sulfoxides bulkier than methyl phenyl sulfoxide. In the present paper we report the synthesis and properties of two new isoreticular, homochiral, porous coordination polymers with longer bridging ligands and different chiral centers $[Zn_2(xdc)(L^*)(dmf)]$, in which xdc = ndc (2,6-naphthalenedicarboxylate) or bpdc (4,4′-biphenyldicarboxylate); L* = chiral (*R*)-mandelate. All of these compounds share the same metal–organic framework topology and other structural features. The enhanced porosity of the mandelate-based polymers allows the enantioselective sorption performance for bulkier chiral guests and selective oxidation of bulkier sulfides (e.g., 2-NaphSMe (2-$C_{10}H_7SMe$) and $PhSCH_2Ph$) that could not be oxidized in the presence of the smaller-pore $[Zn_2(bdc)(lac)(dmf)]$. Furthermore, we carried out theoretical ab initio calculations of host–guest interactions between host frameworks and chiral substrates, which not only fully support the experimental data, but provide important insights into the nature of enantioselective discrimination and further developments of chiral porous absorbents for the fine purification of chiral molecules.

Results and Discussion

Synthesis and structure: The homochiral porous metal–organic frameworks were prepared by heating Zn^{II} nitrate, the bridging ligand (H_2ndc or H_2bpdc) and chiral (*R*)-mandelic acid (H_2man) in DMF. The colorless crystals were obtained and their structures were established by single-crystal X-ray diffraction. The yield of crystalline compounds $[Zn_2(ndc)\{(R)\text{-man}\}(dmf)]\cdot 3\,DMF$ (**1**) and $[Zn_2(bpdc)\{(R)\text{-man}\}(dmf)]\cdot 2\,DMF$ (**2**) was moderately good; the phase purity was confirmed by powder X-ray diffraction and the guest composition was refined by elemental analysis and TG analysis. According to the results from X-ray diffraction, there are two types of Zn^{2+} centers in the polymeric structures **1** and **2**, each in a trigonal-bipyramidal environment and coordination number five, similar to that we found previously in the zinc(II) terephthalate lactate structure $[Zn_2(bdc)\{(S)\text{-lac}\}(dmf)]\cdot DMF$ (**3**).[10] The Zn^{2+} ions, chiral man^{2-} ligands, and carboxylate groups of the bridging ligands ($bpdc^{2-}$ or ndc^{2-}) form one-dimensional chiral chains along the *a* axis (Figure 1 a). These chiral chains could be considered as secondary building units, which are interlinked by linear spacers ($bpdc^{2-}$ or ndc^{2-}) into a three-dimensional, polymeric, non-interpenetrated, coordination network with an open architecture. The geometry of the pores could be approximated as rhombic channels, running along the same *a* direction and intersecting with smaller windows. The pendant phenyl groups of the chiral mandelate anions occupy the interstitial space, providing a chiral environment for the porous structures **1** and **2**. It is worth mentioning that the mandelate ligands in the these metal–organic frameworks participate as dianions owing to the hydroxyl group deprotonation, making these frameworks charge-neutral. The pore sizes, estimated from the X-ray single crystal data, are about 6×10 Å for **1** and 4×14 Å for **2**; however, the passages of the channels are partially blocked by the coordinated DMF ligands. These numbers are, as expected, notably higher than the 5 Å pore diameter in zinc(II) terephthalate lactate **3**. The size of the smaller side windows are 4×4 Å for **1** and 5×7 Å for **2**. Interestingly, the rhombic section of the channels for **1** is notably wider than for **2**, probably due to some steric repulsion of the ndc and man ligands (Figure 1 b and c). Due to this effect, the accessible volumes for the guest-free frameworks $[Zn_2(xdc)(man)(dmf)]$ are nearly identical and were calculated to be 60 % for **1** and 59 % for **2**, despite the differences in the length of the dicarboxylate linkers. Both numbers are higher than 40 % for **3**, which is also in good agreement with elongation of the bridging ligand used for the synthesis of **1** and **2.** The open space in the porous structures of the crystalline compounds is occupied by coordinated and guest DMF molecules. Due to the disorder in the spacious pores of metal–organic coordination polymer **1**, the exact positions of the DMF molecules were not established from the X-ray diffraction experiment. In contrast, we successfully located all DMF molecules in the narrower pores of **2**. In any case, the refined compositions of solvent molecules for **1** and **2** were independently calculated and confirmed from the elemental and thermogravimetric analysis, assuming DMF as the only guest.

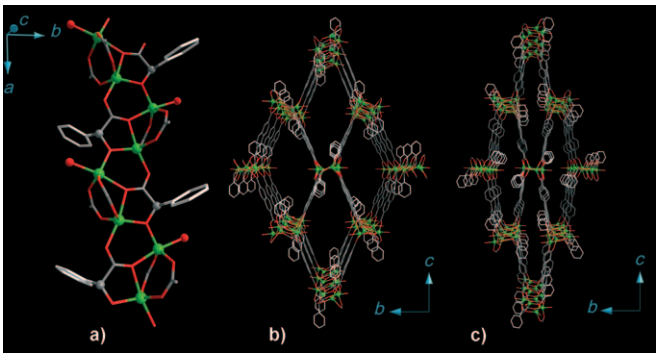

Figure 1. a) The structure of the chiral chain as a secondary building unit; b) and c) the perspective view along the chiral chains of the crystal structures of microporous homochiral coordination polymers 1 and 2, respectively. Legend: Zn: green, O: red, C: grey. Hydrogen atoms and coordinated dmf molecules (except the O atoms, shown by red spheres) are omitted for clarity. Phenyl groups of the chiral mandelate ligand are white.

Stereoselective sorption and catalytic behavior: The capability of stereoselective sorption of organic molecules is one of the most challenging properties of chiral metal–organic frameworks. Recently, we have shown that zinc(II) terephthalate lactate **3** absorbs small alkyl aryl sulfoxides with up to 60% *ee*.[10,11a] To further explore the chiral porous metal–organic structures **1** and **2**, we performed stereoselective sorption experiments (Table 1). As one could expect, the larger pore sizes of **1** and **2** allow for effective absorption of the bulkier sulfoxide guest molecules, which was not possible for **3**. Indeed, coordination polymers **1** and **2** have been found to accommodate most of the alkyl aryl sulfoxides tested (PhSOMe, PhSO*i*Pr, 2-NaphSOMe (2-$C_{10}H_7$SOMe), see Table 1), demonstrating reasonable total sorption values (from 0.3 to 0.7 guest sulfoxide molecules per formula unit), in contrast to the earlier published results for **3**, which could only efficiently accommodate the least bulky sorbates PhSOMe and PhSO*i*Pr (Table 1). The porous chiral structure **1** with ndc^{2-} linkers and a smaller pore size also demonstrates moderate-to-good sorption with low-to-moderate enantioselectivities in the cases of PhSOMe (19% *ee*) and 2-NaphSOMe (17% *ee* in CH_3CN and 31% *ee* in CH_2Cl_2) (Table 1, entries 6, 10, and 11). Surprisingly, for the sorption of PhSO*i*Pr, polymer **1** showed a rather moderate enantioselectivity in CH_2Cl_2 and a record *ee* value of 62% in CH_3CN (Table 1, entries 7, 8; the apparent stereoselectivity factor $K_R/K_S \approx 7$), exceeding that for the sorption of PhSOMe in **3** (Table 1, entry 1).

The larger pore structure **2** readily absorbed 2-NaphSOMe, with moderate stereoselection (27% *ee*, Table 1, entry 16), while for the sorption of other substrates (either smaller sulfoxide PhSOMe, PhSO*i*Pr or bulkier $PhSOCH_2Ph$), it demonstrated much lower sorption and lower stereopreference (Table 1, entries 12–15). In fact, $PhSOCH_2Ph$ showed small sorption on both **1** and **2**, evidencing a poor accommodation of this substrate inside the chiral pores.

We can conclude that the inner pore structure of **1** is more appropriate for the sorption of sulfoxides, demonstrating a better sorption behavior with higher stereopreference. It should be noted that homochiral metal–organic frameworks **1** and **2**, with *R* configuration of the chiral centers (mandelic acid), in most cases demonstrate a higher affinity toward the *R* isomers of sulfoxides (exceptions are (*S*)-PhSOMe for **1** and (*S*)-PhSO*i*Pr for **2**). In a similar manner, stereoselective sorption on **3**, featuring the (*S*)-lactate chiral centers, showed higher sorption of (*S*)-sulfoxides (Table 1, entries 1, 2).

Table 1. Enantioselective sorption of alkyl aryl sulfoxides over homochiral coordination polymers **1–3**.[a]

	Framework	Pore size [Å]	Sulfoxide	Solvent	$c_{sulfoxide}$ [M]	Sorption [molecules per Zn_2]	*ee* [%][b]
1	**3**[c]	5×5	PhSOMe	CH_2Cl_2	0.034	0.30	60 (*S*)
2	**3**[c]	5×5	PhSO*i*Pr	CH_2Cl_2	0.06	0.25	54 (*S*)
3	**3**[c]	5×5	2-NaphSOMe	CH_2Cl_2	0.08	0.13	–[d]
4	**3**[c]	5×5	$PhSOCH_2Ph$	CH_2Cl_2	0.09	0	–[d]
5	**3**[c]	5×5	sulforaphane prec.[e]	CH_2Cl_2	0.068	0.65	20 (*R*)
6	**1**	6×10	PhSOMe	CH_2Cl_2	0.08	0.36	19 (*S*)
7	**1**	6×10	PhSO*i*Pr	CH_3CN	0.08	0.51	62 (*R*)
8	**1**	6×10	PhSO*i*Pr	CH_2Cl_2	0.08	0.16	15 (*R*)
9	**1**	6×10	$PhSOCH_2Ph$	CH_2Cl_2	0.08	0.13	0
10	**1**	6×10	2-NaphSOMe	CH_3CN	0.08	0.72	17 (*R*)
11	**1**	6×10	2-NaphSOMe	CH_2Cl_2	0.08	0.48	31 (*R*)
12	**2**	4×14	PhSOMe	CH_2Cl_2	0.08	0.08	12 (*R*)
13	**2**	4×14	PhSO*i*Pr	CH_3CN	0.08	0.13	7 (*S*)
14	**2**	4×14	PhSO*i*Pr	CH_2Cl_2	0.08	0.02	–[d]
15	**2**	4×14	$PhSOCH_2Ph$	CH_2Cl_2	0.08	0.05	0
16	**2**	4×14	2-NaphSOMe	CH_3CN	0.08	0.44	27 (*R*)

[a] Entries 1, 2, 4 have been reported earlier.[10] [b] Absolute configuration of the adsorbed sulfoxide is given in parentheses. [c] [Zn_2(bdc)(lac)(dmf)]·DMF chiral porous framework was used. [d] *ee* not measured because of low sulfoxide concentration. [e] Sulforaphane precursor $CH_3SO(CH_2)_4OH$ was used.

We also point out that in all cases the enantioselective inclusion of sulfoxides into the chiral pores of the metal–organic frameworks was accompanied by a partial removal of DMF guest molecules (Supporting Information). Therefore, the observed phenomenon is best regarded as guest exchange sorption.

Chiral sulfoxides constitute an important class of biologically active compounds and therapeutic drugs.[15] For example, the active component of Nexium™, one of the world's most popular drugs with $7.8 billion worldwide sales in 2008,[15d] is a magnesium salt of chiral sulfoxide (*S*)-omeprasole. Another important example is sulforaphane, an anticancer and antimicrobial compound,[15b–c] which could be found in some cruciferous vegetables.

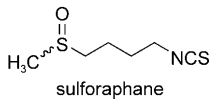

sulforaphane

Since sulforaphane itself is unstable under the experimental conditions, the sorption of its precursor $CH_3SO(CH_2)_4OH$ onto zinc(II) terephthalate lactate **3** was probed. The sulforaphane precursor demonstrated a high sorption along with encouraging enantioselectivity of 20% *ee* (entry 5). Although these numbers are not very high themselves, they clearly suggest that homochiral porous coordination polymers could be utilized for the stereoselective sorption and fine purification of important bioactive molecules including drugs. We believe that with all the structural design versatility of coordination polymers, the stereoselective sorption performance could be improved in the future to a level acceptable for real industrial applications in fine chiral separation and purification.

In previous work we reported the catalytic properties of the zinc(II) terephthalate lactate **3**: it catalyzed the highly selective heterogeneous oxidation of thioethers to sulfoxides with H_2O_2 with remarkable size selectivity;[10,11a] however, the small pore size allowed the oxidation of only rather small substrates (see reference [10] and Table 2). The higher pore size of **1** and **2** (with respect to **3**) is the crucial point determining the difference in their catalytic behaviors. While **3** effectively catalyzed the oxidation of the small substrate PhSMe and displayed virtually no activity towards the oxidation of $PhSCH_2Ph$ (Table 2, entries 1-3), the larger-pore polymers **1** and **2** afforded sulfoxides with high selectivity on the oxidation of the much bulkier substrates 2-NaphSMe and $PhSCH_2Ph$, the remarkable chemoselectivity being retained (Table 2, entries 4–7). Thus, the presented Zn-based porous polymers constitute a family of catalysts for chemo- and size-selective oxidation of sulfides to sulfoxides with H_2O_2. The catalytic systems presented are based on biocompatible metal and chirality sources and use an environmentally benign oxidant; furthermore, they are substantially free from the major disadvantage of sulfoxidation catalysts: insufficient chemoselectivity. To the best of our knowledge, compounds **1–3** are the first heterogeneous Zn-based selective sulfoxidation catalysts.

Table 2. Sulfide oxidation with 30% aqueous H_2O_2 over **1**, **2** and **3**.

	Sulfide	Framework	Pore size [Å]	[S]/[Zn]/[H_2O_2]	Solvent	Conversion [%]	Selectivity [%]
1	PhSMe	**3**	5×5	3:1:9	CH_3CN	92	100
2	PhSMe	**3**	5×5	10:1:15	CH_3CN	94	98
3	$PhSCH_2Ph$[a]	**3**	5×5	2:1:4	CH_2Cl_2	3	–
4	2-NaphSMe	**1**	6×10	12.5:1:25	CH_3CN	78	99
5	$PhSCH_2Ph$	**1**	6×10	12.5:1:25	CH_3CN	70	99
6	2-NaphSMe	**2**	4×14	12.5:1:25	CH_3CN	57	98
7	$PhSCH_2Ph$	**2**	4×14	12.5:1:25	CH_3CN	78	98.5

[a] Urea hydroperoxide was used as the oxidant, [S]:[Zn] = 2:1.

DFT modeling of the enantioselective sorption: In order to investigate the nature of stereoselectivity as well as to obtain quantitative data of the host–guest interaction energies, we carried out extensive first-principles calculations. The selected methods are used to calculate the accurate adsorption energies (E_{ads}) as the difference between the binding energy of the adsorbed system ($E_{host+guest}$) and those of the empty metal–organic framework (E_{host}) and free guest molecules (E_{guest}) [Eq. (1)].

$$E_{ads} = E_{host+guest} - (E_{host} + E_{guest}) \quad (1)$$

A negative value of E_{ads} means that the corresponding adsorption state is thermodynamically favorable. Recently, we have successfully applied the present theoretical approach to explain the high sorption selectivity of acetylene from a C_2H_2/CO_2 gas mixture on Cu^{II} containing a microporous coordination polymer.[16] In all cases, the optimizations of both atomic positions and cell volume were performed.

At a first step, using the [Zn_2(bdc){(*S*)-lac}(dmf)] chiral metal–organic framework, we investigated the sorption of the *S* and *R* optical isomers of methyl phenyl sulfoxide $PhSOCH_3$. The optimized geometries and charge density isosurfaces are shown in Figure 2. A charge density isosurface conveniently demonstrates the process of interaction between the porous coordination polymer host and the encapsulated molecules. Starting from the same guest location in the channel of porous frameworks for both isomers, a full geometry optimization was carried out. Our calculations show a large difference in absorption energies between the *S* and *R* isomers of $PhSOCH_3$. The optimization shows that only the *S* isomer can be stabilized in the host framework due to the negative value (-1.568 kcal mol^{-1}) of the calculated heat of adsorption (see Figure 2a). The charge accumulation and hence the formation of a weak C–H···O hydrogen bond between the H atom of the methyl group in the pendant DMF ligand and the O atom of (*S*)-$PhSOCH_3$ has been observed. The calculated distance between the oxygen atom of $PhSOCH_3$ and the DMF hydrogen atom was found to be 2.10 Å. Such interaction is missing in the case of the *R* isomer as shown in Figure 2b. In contrast, a repulsive interaction between the methyl group of guest $PhSOCH_3$ and the DMF ligand has been found. As a result, the heat of adsorption value is positive ($+9.432$ kcal mol^{-1}), indicating that the host chiral framework could not effectively accommodate this optical isomer. In order to realize a C–H···O bond and avoid the repulsion, we rotated the (*R*)-$PhSOCH_3$ molecule by 180° inside the host channel. From this starting configuration, a geometry in which the weak C–H···O hydrogen bond between the H atom of the methyl group in the DMF

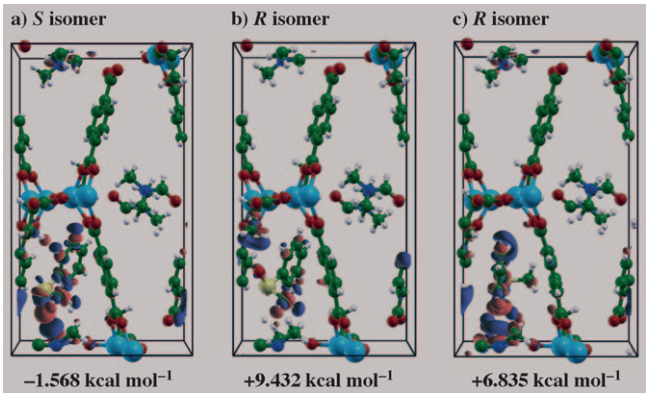

Figure 2. Charge density isosurface of the host-guest structure for a) the *S* isomer of $PhSOCH_3$; b) and c) the two different orientations of the *R* isomer of $PhSOCH_3$. Red represents an accumulation of electrons and blue a depletion of electrons.

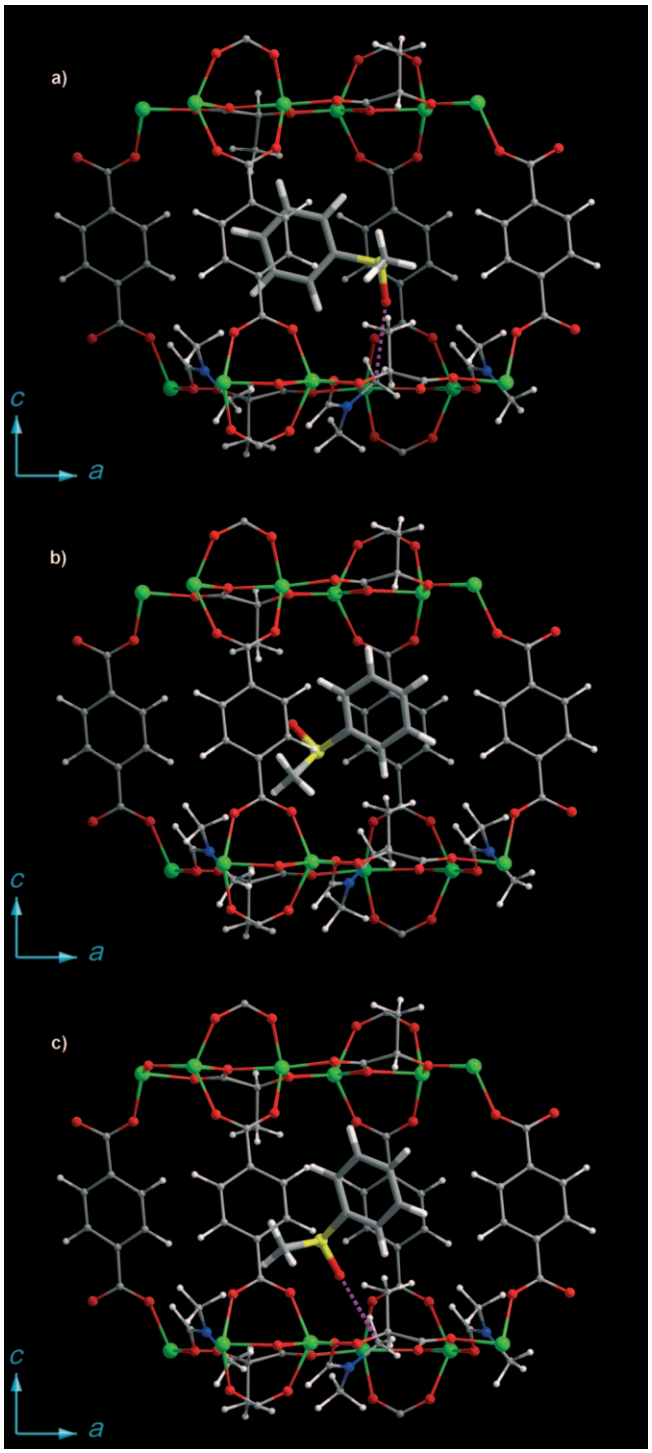

Figure 3. Presentation of the optimized chiral methyl phenyl sulfoxide guest orientations inside the pores of the $[Zn_2(bdc)(lac)(dmf)]$ framework: a) (*S*)-$PhSOCH_3$; b) (*R*)-$PhSOCH_3$; c) alternative orientation of (*R*)-$PhSOCH_3$. Legend: Zn: green, O: red, C: grey, H: white, N: blue, S: yellow. Guest molecules are shown as a thick wire model, while the purple dotted lines indicate C–H···O hydrogen-bond interactions.

ligand and the O atom of the *R* isomer can also be produced. The optimized geometry is shown in Figure 2c. For this optimized picture, the C–H···O bond has a calculated distance of 2.37 Å. However, in the latter configuration, repulsive interactions between the guest methyl group and the neighboring DMF ligand as well as between the phenyl rings of the guest and host framework (bdc) have been observed. As a result, the adsorption of (*R*)-methyl phenyl sulfoxide is still unfavorable due to the positive value of the interaction energy ($+6.835\ kcal\,mol^{-1}$). The large difference in energy clearly supports the pronounced sorption enantioselectivity by zinc(II) terephthalate lactate toward the *S* optical isomers of small chiral sulfoxides, which was reported previously.[10,11a]

Moreover, such theoretical calculations provide an explanation of the nature of multiple host–guest interactions responsible for the stereoselective recognition. Figure 3 shows the calculated orientations of $PhSOCH_3$ guest inside the pores of host **3**.

Using the same strategy, we probed the sorption ability of the sulforaphane precursor $CH_3SO(CH_2)_4OH$ onto the porous host framework **3**. Figure 4 shows the calculated orientations of the chiral $CH_3SO(CH_2)_4OH$ guest inside the

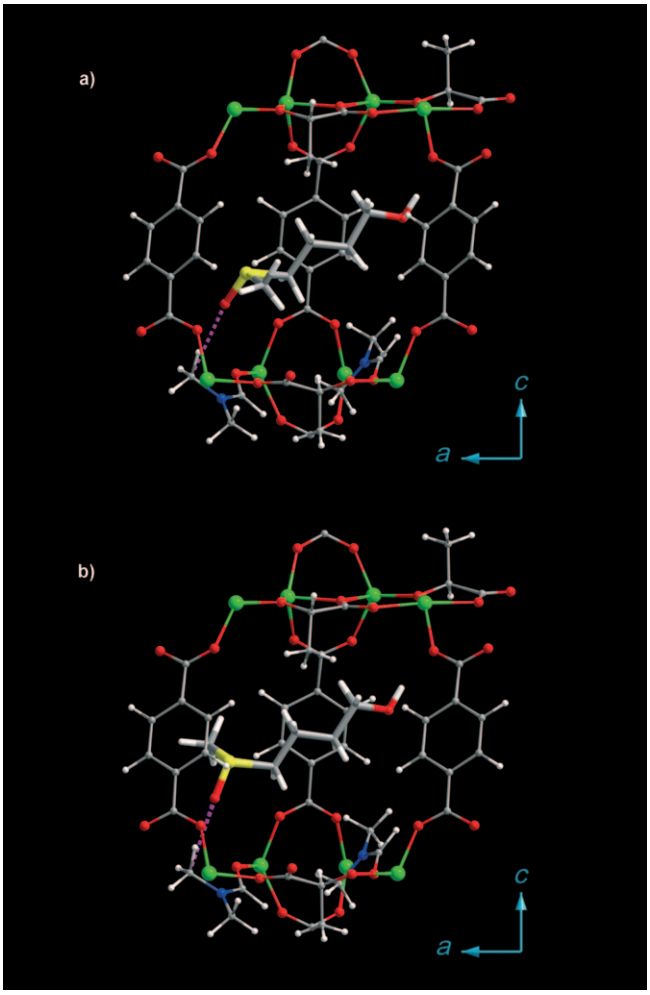

Figure 4. Presentation of the optimized chiral sulforaphane precursor $CH_3SO(CH_2)_4OH$ orientations inside the pores of $[Zn_2(bdc)(lac)(dmf)]$ framework: a) *S* isomer; b) *R* isomer. Legend: Zn: green, O: red, C: grey, H: white, N: blue, S: yellow. Guest molecules are shown as a thick wire model, while the purple dotted lines indicate C–H···O hydrogen-bond interactions.

pores of the chiral host. In this case, both of the optical isomers of sulforaphane show a favorable adsorption trend due to negative value of the calculated heat of adsorption. However, a difference in the adsorption energy has been observed. The interaction energy of the *R* isomer with the host lattice is $-5.442\ kcal\,mol^{-1}$, which is larger than the corresponding value for the *S* isomer of $-3.415\ kcal\,mol^{-1}$. The charge density isosurface (see Figure SI_6 in the Supporting Information) indicates a redistribution of charge along the carbon chain of guest molecules and the formation of C–H···O hydrogen bonds in both cases. However, the absence of a bulky phenyl ring in $CH_3SO(CH_2)_4OH$ results in reduced repulsions between the guest and the host wall, which is the case for (*R*)-methyl phenyl sulfoxide. These calculations also fully support the experimental data; however, the smaller energy difference predictably results in a reduction of enantioselectivity for the sulforaphane precursor (Table 1).

It should be noted that the presence of a coordinated DMF ligand is one of the key factors in stereoselective recognition due to the formation of weak hydrogen bond through the oxygen atom of the sulfoxide. The thermally activated metal–organic framework without pendant DMF ligands will have a large pore size and will be able to accommodate larger sulfoxide molecules. However, in this case, the main stabilization factor will be based on weaker van der Waals interaction and, hence, such coordination polymer should, in general, demonstrate poorer stereopreference, as has been shown experimentally for the activated $[Zn_2(bdc)(lac)(dmf)]\cdot x$DMF ($x \leq 0.4$) framework.[10]

Conclusion

Using the rational modular approach, two new homochiral porous metal–organic coordination polymers ($[Zn_2(ndc)\{(R)\text{-man}\}(dmf)]\cdot 3$DMF and $[Zn_2(bpdc)\{(R)\text{-man}\}(dmf)]\cdot 2$DMF) have been synthesised. These structures share the same topological features as the previously reported zinc(II) terephthalate lactate $[Zn_2(bdc)\{(S)\text{-lac}\}(dmf)]\cdot$DMF framework, but have larger pores and opposite absolute configuration of the chiral centres, thus giving examples of rational fine-tuning of essential structural properties in porous homochiral coordination polymers. The larger pores size and different chiral centers structure result in differing stereoselective sorption properties: the new polymers effectively and stereoselectively accommodate bulkier guest molecules than the parent $[Zn_2(bdc)\{(S)\text{-lac}\}(dmf)]\cdot$DMF, while the parent framework demonstrates higher sorption and enantioselectivity toward smaller chiral drug precursor. Furthermore, new chiral compounds are capable of catalyzing a highly selective oxidation of bulkier sulfides (2-NaphSMe and $PhSCH_2Ph$) that could not be oxidized in the presence of the smaller pore $[Zn_2(bdc)\{(S)\text{-lac}\}(dmf)]\cdot$DMF. Importantly, the sorption of two different guest molecules (*R* and *S* isomers) into the chiral pores of $[Zn_2(bdc)\{(S)\text{-lac}\}(dmf)]$ was modeled by using ab initio calculations; these results provided a qualitative explanation for the observed sorption enantioselectivity. In particular, the high stereopreference is accounted for by the presence of coordinated inner pore DMF molecule, which forms a weak C–H···O bond between the DMF methyl group and the (*S*)-$PhSOCH_3$ sulfinyl group.

Experimental Section

Materials and methods: All starting chemicals were used as purchased without additional purification. Synthesis, sorption, and catalysis experiments were performed in analytical grade organic solvents. ^{1}H NMR spectra were recorded on a Bruker AVANCE 400 MHz spectrometer at 400.13 MHz, using 5 mm cylindrical tubes. Chemical shifts were referenced to internal reference TMS, with positive values in the low-field direction. The enantiomeric excess (*ee*) values for the sulfoxides were measured by ^{1}H NMR spectroscopy with $[Eu(hfc)_3]$ (hfc = 3-(heptafluoropropylhydroxymethylene)-(+)-camphorate) as a chiral shift reagent in CCl_4 or $CCl_4/CDCl_3$, as reported in references [10,11a]. The enantiomeric excess (*ee*) values for the sulphoraphane precursor $CH_3SO(CH_2)_4OH$ were measured on a KRUSS P3002RS polarimeter. The elemental CHN analysis was carried out on EURO EA 3000.The powder diffraction data were collected using Stoe Stadi and Siemens D5000 diffractometers (λ = 1.54056 Å). The IR spectra in KBr pellets were recorded on a Scimitar FTS 2000 spectrophotometer. The TGA plots were recorded on the TG 209 F1 apparatus in an Ar atmosphere at a heating rate of $10°\,min^{-1}$.

General sorption procedure: For the sorption experiments, porous coordination polymers were used as prepared, that is, $[Zn_2(ndc)(man)(dmf)]\cdot 3$DMF (**1**), $[Zn_2(bpdc)(man)(dmf)]\cdot 2$DMF (**2**) and $[Zn_2(bdc)(lac)(dmf)]\cdot$DMF (**3**). A racemic sulfoxide (0.05–0.1 mmol) was dissolved in CH_2Cl_2 (1 mL), and the appropriate powdered coordination polymer (20–40 mg) was added. After stirring the mixture for 16 h at room temperature, the crystalline adsorbent was collected by filtration and flushed with hexane (1 mL), which does not wash out the adsorbed compounds. The solid was extracted with methanol (3×3 mL) to retrieve the adsorbed sulfoxide, and then the solvent was removed in vacuo. The remaining sulfoxide was dissolved in CCl_4 or $CCl_4/CDCl_3$ and transferred into an NMR tube.

General oxidation procedure: A mixture of a sulfide (0.15 mmol), the appropriate coordination polymer (10 mg), and an oxidant (H_2O_2, 1–2 equiv with respect to the sulfide) dissolved in the appropriate solvent (1.5 mL) was stirred at room temperature for 16 h. Then, the solid catalyst was collected by filtration, and the adsorbed sulfoxide was extracted with methanol (3×3 mL). The extract and filtrate were combined, the volatiles were removed in vacuo, and the composition of the reaction products and the enantiomeric excess were measured by ^{1}H NMR spectroscopy with the chiral shift reagent $[Eu(hfc)_3]$ in CCl_4, as in references [10,11a].

Synthesis of $[Zn_2(ndc)\{(R)\text{-man}\}(dmf)]\cdot 3$DMF (1): $Zn(NO_3)_2\cdot 6H_2O$ (4.5 g, 15 mmol), 2,6-naphthalenedicarboxylic acid (1.62 g, 7.5 mmol) and (*R*)-mandelic acid (1.47 g, 9.67 mmol) were dissolved in DMF (300 mL) and heated at 80 °C for 4 days. After this time bundles of block-shaped colorless crystals of **1** were collected, washed with DMF (3×15 mL) and air-dried for several hours. Yield: 3.72 g (≈58 %); elemental analysis calcd (%) for $C_{32}H_{40}N_4O_{11}Zn_2$: C 48.8, H 5.1, N 7.1; found: C 48.5, H, 5.0, N, 7.2; thermogravimetric analysis data: found solvent weight loss for **1**: 39.0 % (37.1 % calculated for 4 DMF).

Synthesis of $[Zn_2(bpdc)\{(R)\text{-man}\}(dmf)]\cdot 2$DMF (2): $Zn(NO_3)_2\cdot 6H_2O$ (600 mg, 2.0 mmol), 4,4′-biphenyldicarboxylic acid (242 mg, 1.0 mmol) and (*R*)-mandelic acid (175 mg, 1.15 mmol) were dissolved in hot DMF (40 mL). The solution was heated in a teflon autoclave for 2 days at 100 °C. Colorless rod-shaped crystals of **2** were collected, washed with DMF (3×10 mL) and air-dried for several hours. Yield: 520 mg (≈70 %); elemental analysis calcd (%) for $C_{31}H_{35}N_3O_{10}Zn_2$: C 50.3, H 4.8, N 5.7; found: C 50.2, H 4.7, N 5.4; thermogravimetric analysis data: found solvent weight loss for **2**: 28.7 % (29.6 % calculated for 3 DMF).

Single-crystal X-ray diffraction: Single-crystal X-ray diffraction data on **1** and **2** were collected on a Bruker X8 Apex CCD diffractometer equipped with an area detector ($Mo_{K\alpha}$, graphite monochromator, ϕ and ω scans). Data collection, frame integration, and data processing were performed with the use of the APEX2 and SAINT program packages.[17] The absorption correction was applied based on the intensities of equivalent reflections with the use of the SADABS program.[17] The structures were solved by direct methods and refined anisotropically (except for the H atoms) by the full-matrix least-squares method using the SHELX-97 program package.[18] Hydrogen atoms were placed geometrically and refined using a rigid model. The unit cell volume of **1** included a large region of disordered solvent that could not be modeled as discrete atomic sites. We employed PLATON/SQUEEZE[19] to calculate the contribution to the diffraction from the solvent region and thereby produced a set of solvent-free diffraction intensities. Furthermore, due to the disordering, it was not possible to locate all the atoms of coordinated dmf molecule in **1**. The final formula of **1** was calculated from the SQUEEZE results (496 *e* per unit cell) combined with elemental analysis data. Crystal data and results of the structure refinements are summarized in Table 3. CCDC-764948 (**1**) and 764949 (**2**) contain the supplementary crystallographic data for this paper. These data can be obtained free of charge from The Cambridge Crystallographic Data Centre via www.ccdc.cam.ac.uk/data_request/cif.

Table 3. Crystal data and structure refinement for **1** and **2**.

	1	**2**
formula	$C_{32}H_{40}N_4O_{11}Zn_2$	$C_{31}H_{35}N_3O_{10}Zn_2$
M_r [g mol^{-1}]	787.42	740.36
T [K]	90(2)	100(2)
crystal system	orthorhombic	orthorhombic
space group	$P2_12_12_1$	$P2_12_12_1$
a [Å]	10.2398(3)	10.1365(2)
b [Å]	15.4892(6)	11.4134(3)
c [Å]	23.7128(8)	29.2794(7)
V [Å^3]	3761.0(2)	3387.39(14)
Z	4	4
ρ_{calcd} [g cm^{-3}]	1.391	1.452
μ [mm^{-1}]	1.335	1.474
$F(000)$	1632	1528
crystal size [mm]	$0.92\times0.32\times0.10$	$0.93\times0.16\times0.03$
θ [°]	2.16–31.18	1.92–26.37
hkl indicies	$-8\le h\le13$	$-12\le h\le8$
	$-16\le k\le21$	$-14\le k\le12$
	$-33\le l\le34$	$-36\le l\le36$
total/unique/observed reflections	25199/9955/6687	18760/6324/5415
R_{int}	0.0327	0.0395
min/max transmission	0.8826/0.3744	0.9571/0.3410
restraints/parameters	30/309	204/416
goodness-of-fit on F^2	0.967	1.034
final R indices	$R_1=0.0462$,	$R_1=0.0373$,
$[I>2\sigma(I)]$	$wR_2=0.1118$	$wR_2=0.0829$
R indices (all data)	$R_1=0.0734$,	$R_1=0.0496$,
	$wR_2=0.1204$	$wR_2=0.0865$
absolute structure parameter	0.050(14)	0.003(12)
largest diff. peak/hole [e Å^{-3}]	1.255/−0.473	0.464/−0.452

Calculations: All DFT calculations were performed using the Vienna Ab Initio Simulation Package (VASP).[20] The generalized gradient corrected PW91 exchange-correlation functional[21] and the all-electron projector augmented wave method[22] were used in order to accurately describe the interaction between the ion and electron. During the optimization procedure, the plane-wave cutoff energy was set to 400 eV and the convergence in energy and force were 10^{-4} eV and 3×10^{-3} eV Å^{-1}, respectively. The interaction energy between the guest molecules and host lattice was evaluated using a higher value of cutoff energy (420 eV). Brillouin zone integrations were performed on a Monkhorst–Pack grid.[23]

Acknowledgements

Financial support from the Russian Foundation for Basic Research (grants 08-03-12007 and 09-03-90414) is gratefully acknowledged. R.V.B., H.M., and Y.K. thank the Information Science Group of IMR, Tohoku University, for their continuous support of the SR11000 Supercomputing System, and the Ministry of Education, Culture, Sports, Science, and Technology of Japan (Grant No. 19651039) for financial support. We are also thankful to Dr. T. M. Briere for carefully reading this manuscript. Moreover D.N.D. gratefully acknowledges the WCU Program through the Korea Science and Engineering Foundation funded by the Ministry of Education, Science and Technology of Korea (Project No. R31-2008-000-10059-0) for the support of this work.

[1] B. Kesanli, W. Lin, *Coord. Chem. Rev.* **2003**, *246*, 305–326.
[2] a) L. Ma, C. Abney, W. Lin, *Chem. Soc. Rev.* **2009**, *38*, 1248–1256; b) K. Ding, Z. Wang, X. Wang, Y. Liang, X. Wang, *Chem. Eur. J.* **2006**, *12*, 5188–5197; c) S. Kitagawa, R. Kitaura, S. Noro, *Angew. Chem.* **2004**, *116*, 2388–2430; *Angew. Chem. Int. Ed.* **2004**, *43*, 2334–2375.
[3] J. S. Seo, D. Wand, H. Lee, S. I. Jun, J. Oh, Y. Jeon, K. Kim, *Nature* **2000**, *404*, 982–986.
[4] a) W. Lin, *MRS Bull.* **2007**, *32*, 544–548; b) K. P. Bryliakov, E. P. Talsi in *Transition Metal Chemistry: New Research* (Eds.: B. Varga, L. Kis), Nova Science Publishers, New York, **2008**, pp. 1–13.
[5] J. C. Leffingwell, *Chirality & Bioactivity I: Pharmacology, Vol. 3*, Leffingwell Reports, **2003**.
[6] V. Farina, J. T. Reeves, C. H. Senanayake, J. J. Song, *Chem. Rev.* **2006**, *106*, 2734–2793.
[7] M. Heitbaum, F. Glorius, I. Escher, *Angew. Chem.* **2006**, *118*, 4850–4881; *Angew. Chem. Int. Ed.* **2006**, *45*, 4732–4762.
[8] a) C.-D. Wu, A. Hu, L. Zhang, W. Lin, *J. Am. Chem. Soc.* **2005**, *127*, 8940–8941; b) M. Banerjee, S. Das, M. Yoon, H. J. Choi, M. H. Hyun, S. M. Park, G. Seo, K. Kim, *J. Am. Chem. Soc.* **2009**, *131*, 7524–7525; c) S.-H. Cho, B. Ma, S. T. Nguyen, J. T. Hupp, T. E. Albrecht-Schmitt, *Chem. Commun.* **2006**, 2563–2565; d) K. Tanaka, S. Oda, M. Shiro, *Chem. Commun.* **2008**, 820–822.
[9] a) D. Bradshaw, T. J. Prior, E. J. Cussen, J. B. Claridge, M. J. Rosseinsky, *J. Am. Chem. Soc.* **2004**, *126*, 6106–6114; b) R.-G. Xiong, X.-Z. You, B. F. Abrahams, Z. Xue, C.-M. Che, *Angew. Chem.* **2001**, *113*, 4554–4557; *Angew. Chem. Int. Ed.* **2001**, *40*, 4422–4425; c) R. Vaidhyanathan, D. Bradshaw, J.-N. Rebilly, J. P. Barrio, J. A. Gould, N. G. Berry, M. J. Rosseinsky, *Angew. Chem.* **2006**, *118*, 6645–6649; *Angew. Chem. Int. Ed.* **2006**, *45*, 6495–6499.
[10] D. N. Dybtsev, A. L. Nuzhdin, H. Chun, K. P. Bryliakov, E. P. Talsi, V. P. Fedin, K. Kim, *Angew. Chem.* **2006**, *118*, 930–934; *Angew. Chem. Int. Ed.* **2006**, *45*, 916–920.
[11] a) A. L. Nuzhdin, D. N. Dybtsev, K. P. Bryliakov, E. P. Talsi, V. P. Fedin, *J. Am. Chem. Soc.* **2007**, *129*, 12958–12959; b) O. R. Evans, H. L. Ngo, W. Lin, *J. Am. Chem. Soc.* **2001**, *123*, 10395–10396.
[12] a) Y. V. Mironov, N. G. Naumov, K. A. Brylev, V. E. Fedorov, K. Hegetschweiler, *Angew. Chem.* **2004**, *116*, 1317–1321; *Angew. Chem. Int. Ed.* **2004**, *43*, 1297–1300; b) Y. V. Mironov, N. G. Naumov, K. A. Brylev, O. A. Efremova, V. E. Fedorov, K. Hegetschweiler, *Russ. J. Coord. Chem.* **2005**, *31*, 269–281.
[13] D. N. Dybtsev, M. P. Yutkin, E. V. Peresypkina, A. V. Virovets, C. Serre, G. Ferey, V. P. Fedin, *Inorg. Chem.* **2007**, *46*, 6843–6845.
[14] J. Perez Barrio, J.-N. Rebilly, B. Carter, D. Bradshaw, J. Bacsa, A. Y. Ganin, H. Park, A. Trewin, R. Vaidhyanathan, A. I. Cooper, J. E. Warren, M. J. Rosseinsky, *Chem. Eur. J.* **2008**, *14*, 4521–4532.
[15] a) A. Kalir, H. H. Kalir in *The Chemistry of Sulfur-Containing Functional Groups* (Eds.: S. Patai, Z. Rappoport), Wiley, New York,

1993, pp. 957–975; b) I. Fernández, N. Khiar, *Chem. Rev.* **2003**, *103*, 3651–3705; c) T. J. Brown, R. F. Chapman, D. C. Cook, T. W. Hart, I. M. McLay, R. Jordan, J. S. Mason, M. N. Palfreyman, R. J. A. Walsh, M. T. Withnall, J.-C. Aloup, I. Cavero, D. Fargen, C. James, S. Mondot, *J. Med. Chem.* **1992**, *35*, 3613–3624; d) various information including drug sales could be found online on http://www.drugs.com/ and http://www.pharmexec.com.

[16] R. Matsuda, R. Kitaura, S. Kitagawa, Y. Kubota, R. V. Belosludov, T. C. Kobayashi, H. Sakamoto, T. Chiba, M. Takata, Y. Kawazoe, Y. Mita, *Nature* **2005**, *436*, 238–241.

[17] Bruker Advanced X-ray Solutions, Bruker AXS Inc, Madison, **2004**.

[18] G. M. Sheldrick, *Acta Crystallogr. Sect. A* **2008**, *64*, 112–122.

[19] A. L. Spek, *J. Appl. Crystallogr.* **2003**, *36*, 7–13.

[20] a) G. Kresse, J. Furthmuller, *Phys. Rev. B* **1996**, *54*, 11169–11186; b) G. Kresse, J. Furthmuller, *Comput. Mater. Sci.* **1996**, *6*, 15–50.

[21] J. P. Perdew, J. A. Chevary, S. H. Vosko, K. A. Jackson, M. R. Pederson, D. J. Singh, C. Fiolhais, *Phys. Rev. B* **1992**, *46*, 6671–6687.

[22] P. E. Blöchl, *Phys. Rev. B* **1994**, *50*, 17953–17979.

[23] H. J. Monkhorst, J. D. Pack, *Phys. Rev. B* **1976**, *13*, 5188–5192.

Received: February 28, 2010
Revised: June 28, 2010
Published online: August 20, 2010

